

# Search for excited charmonium states in $e^+e^-$ annihilation at

$$\sqrt{s} = 10.6 \text{ GeV}$$

Kui-Yong Liu <sup>(a,b)</sup>, Zhi-Guo He <sup>(a)</sup>, and Kuang-Ta Chao <sup>(a,c)</sup>

*(a) Department of Physics, Peking University, Beijing 100871, China*

*(b) Department of Physics, Liaoning University, Shenyang 110036, China*

*(c) China Center of Advanced Science and Technology (World Laboratory), Beijing 100080, China*

## Abstract

We suggest searching for excited charmonium states in  $e^+e^-$  annihilation via double charmonium production at  $\sqrt{s} = 10.6$  GeV with  $B$  factories, based on a more complete leading order calculation including both QCD and QED contributions for various processes. In particular, for the  $C=+$  states, the  $\chi_{c0}(nP)$  ( $n=2,3$ ) and  $\eta_c(mS)$  ( $m=3,4$ ) may have appreciable potentials to be observed; while for the  $C=-$  states, the  $\eta_c h_c$  production and especially the  $\chi_{c1} h_c$  production might provide opportunities for observing the  $h_c$  with higher statistics in the future. A brief discussion for the X(3940) observed in the double charmonium production is included.

PACS numbers: 12.40.Nn, 13.85.Ni, 14.40.Gx

## I. INTRODUCTION

Charmonium spectroscopy has become a challenging topic in hadron physics and QCD, because of the recent findings of possible new charmonium states (for recent experimental and theoretical reviews and discussions, see e.g. [1, 2, 3, 4] and references therein). Among others, for the puzzling state X(3872), possible assignments of e.g. the  $2^3P_1$  and  $1^2D_1$  charmonium states and the charm-molecule have been suggested (see, e.g.[5] for a comprehensive review), and it will be helpful to search for those states in other experiments and to clarify these assignments; The measured mass splitting between  $\psi(2S)$  and  $\eta_c(2S)$  is about 50 MeV, which is smaller than some theoretical predictions, and it is certainly useful to search for the  $\eta_c(3S)$  to see what will be the mass splitting between the  $\psi(3S)$ , which could be the observed  $\psi(4040)$ , and the  $\eta_c(3S)$ . This may be particularly interesting since according to some potential model calculations the  $\eta_c(3S)$  could lie above 4040 MeV (see, e.g. in [6] the mass of  $\eta_c(3S)$  is predicted to be 4060 MeV). And the  $\psi(3S)$  mass could actually be lowered by coupling to the nearby  $D^*\bar{D}^*$  decay channels (note that the energy level spacing between  $\psi(3S) = \psi(4040)$  and  $\psi(2S) = \psi(3686)$  is smaller than that between  $\psi(4S) = \psi(4414)$  and  $\psi(3S) = \psi(4040)$ , which is in contradiction with potential model calculations unless the coupled channel effects are considered or the assignments for  $\psi(3S) = \psi(4040)$  and  $\psi(4S) = \psi(4414)$  are incorrect. The mass spectrum of excited charmonium states will certainly provide important information on interquark forces and color confinement. In addition, studies of the decay and production of these states will also be very important in understanding the underlying theory of strong interaction –perturbative and nonperturbative QCD in view of many outstanding puzzles in charmonium physics.

$B$  meson decays have proven to be very useful processes to find new charmonium states. Aside from the  $B$  meson decay,  $e^+e^-$  annihilation at  $\sqrt{s} = 10.6$  GeV could also be a very useful process in finding the excited charmonium states, since the recent Belle experiments [7, 8] have found unusually strong signals for the double charmonium production from the  $e^+e^-$  continuum, e.g.,  $e^+e^- \rightarrow J/\psi\eta_c, J/\psi\chi_{c0}, J/\psi\eta_c(2S)$  and  $e^+e^- \rightarrow \psi(2S)\eta_c, \psi(2S)\chi_{c0}, \psi(2S)\eta_c(2S)$ . Theoretically, the calculated cross sections for these processes based on the leading order Non-Relativistic QCD(NRQCD) (or more generally perturbative QCD (pQCD)) are about an order of magnitude smaller than the experiments [9, 10, 11]. This is a big issue in charmonium physics and NRQCD, and it still remains to be further clarified

though many considerations are suggested to understand the large production rates in both exclusive and inclusive charmonium production via double charm pairs in  $e^+e^-$  annihilation [12] (the theoretical predictions for the inclusive  $J/\psi c\bar{c}$  production cross section with the color-singlet [13, 14, 15] as well as color-octet[16] contributions are also much smaller than the Belle data). Despite of these disagreements, however, we find that the calculated relative rates of the double charmonium production processes are roughly compatible with the Belle data (e.g. the production cross sections of  $\eta_c$ ,  $\eta_c(2S)$ , and  $\chi_{c0}$  associated with  $J/\psi$  and  $\psi(2S)$  are much larger than that of  $\chi_{c1}$  and  $\chi_{c2}$ ). So, we may use the same method as in our previous work to calculate the production rates for the excited charmonium states in  $e^+e^-$  annihilation into double charmonia, but mainly pay attention to the relative rates for these production processes. We hope the calculation will make sense in predicting the relative production rates for those excited charmonium states, and can be tested by experiments. This will be useful not only in the search for those excited charmonium states, but also in understanding the production mechanism itself. If the predicted relative production rates turn out to be consistent with experiments, it is likely that the NRQCD factorization treatment for these processes probably still makes sense and only an overall enhancement factor is needed and should be clarified in further theoretical considerations (including QCD radiative corrections, relativistic corrections, and other nonperturbative QCD effects). In the last section we will have a discussion on recent developments in this regard. In the following, we will calculate the leading order production cross sections for various excited charmonium states in  $e^+e^-$  annihilation at  $\sqrt{s} = 10.6$  GeV in the same way as in [10].

## II. FORMULAS AND CALCULATIONS

Following the NRQCD factorization formalism[17], the scattering amplitude of double charmonia production can be described as

$$\begin{aligned}
\mathcal{A}(a + b \rightarrow Q\bar{Q}(^{2S_\psi+1}L_{J_\psi})(p_3) + Q\bar{Q}(^{2S+1}L_J)(p_4)) &= \sqrt{C_{L_\psi}}\sqrt{C_L} \sum_{L_\psi z S_\psi z} \sum_{s_1 s_2} \sum_{jk} \sum_{L_z S_z} \sum_{s_3 s_4} \sum_{il} \\
&\times \langle s_1; s_2 | S_\psi S_{\psi z} \rangle \langle L_\psi L_{\psi z}; S_\psi S_{\psi z} | J_\psi J_{\psi z} \rangle \langle 3j; \bar{3}k | 1 \rangle \\
&\times \langle s_3; s_4 | SS_z \rangle \langle LL_z; SS_z | JJ_z \rangle \langle 3l; \bar{3}i | 1 \rangle \\
&\times \begin{cases} \mathcal{A}(a + b \rightarrow Q_j(\frac{p_3}{2}) + \bar{Q}_k(\frac{p_3}{2}) + Q_l(\frac{p_4}{2}) + \bar{Q}_i(\frac{p_4}{2})) & (L = S), \\ \epsilon_\alpha^*(L_Z) \mathcal{A}^\alpha(a + b \rightarrow Q_j(\frac{p_3}{2}) + \bar{Q}_k(\frac{p_3}{2}) + Q_l(\frac{p_4}{2}) + \bar{Q}_i(\frac{p_4}{2})) & (L = P), \end{cases}
\end{aligned} \tag{1}$$

where  $\langle 3j; \bar{3}k | 1 \rangle = \delta_{jk}/\sqrt{N_c}$ ,  $\langle 3l; \bar{3}i | 1 \rangle = \delta_{li}/\sqrt{N_c}$ ,  $\langle s_1; s_2 | S_\psi S_{\psi z} \rangle$ ,  $\langle s_3; s_4 | SS_z \rangle$ ,  $\langle L_\psi L_{\psi z}; S_\psi S_{\psi z} | J_\psi J_{\psi z} \rangle$  and  $\langle LL_z; SS_z | JJ_z \rangle$  are respectively the color-SU(3), spin-SU(2), and angular momentum Clebsch-Gordon coefficients for  $Q\bar{Q}$  pairs projecting out appropriate bound states.  $\mathcal{A}(a + b \rightarrow Q_j(\frac{p_3}{2}) + \bar{Q}_k(\frac{p_3}{2}) + Q_l(\frac{p_4}{2}) + \bar{Q}_i(\frac{p_4}{2}))$  is the scattering amplitude for double  $Q\bar{Q}$  production and  $\mathcal{A}^\alpha$  is the derivative of the amplitude with respect to the relative momentum between the quark and anti-quark in the bound state. The coefficients  $C_{L_\psi}$  and  $C_L$  can be related to the radial wave function of the bound states or its derivative with respect to the relative spacing as

$$C_s = \frac{1}{4\pi} |R_s(0)|^2, \quad C_p = \frac{3}{4\pi} |R'_p(0)|^2. \tag{2}$$

We introduce the spin projection operators  $P_{SS_z}(p, q)$  as[18, 19]

$$P_{SS_z}(p, q) \equiv \sum_{s_1 s_2} \langle s_1; s_2 | SS_z \rangle v(\frac{p}{2} - q; s_1) \bar{u}(\frac{p}{2} + q; s_2). \tag{3}$$

Expanding  $P_{SS_z}(P, q)$  in terms of the relative momentum  $q$ , we get the projection operators and their derivatives, which will be used in our calculation, as follows

$$P_{1S_z}(p, 0) = \frac{1}{2\sqrt{2}} \not{\epsilon}^*(S_z)(\not{p} + 2m_c), \tag{4}$$

$$P_{00}(p, 0) = \frac{1}{2\sqrt{2}} \gamma_5(\not{p} + 2m_c), \tag{5}$$

$$P_{00}^\alpha(p, 0) = \frac{1}{2\sqrt{2}m_c} \gamma^\alpha \gamma_5 \not{p} \quad (6)$$

$$P_{1S_z}^\alpha(p, 0) = \frac{1}{4\sqrt{2}m_c} [\gamma^\alpha \not{\epsilon}^*(S_z)(\not{p} + 2m_c) - (\not{p} - 2m_c) \not{\epsilon}(S_z)\gamma^\alpha]. \quad (7)$$

We then get the following expressions and numerical results for various processes of double charmonium production in  $e^+e^-$  annihilation at  $\sqrt{s} = 10.6$  GeV. In the calculation of the short distance coefficients, the quark and anti-quark are all on mass shell, and the meson masses are taken to be  $m_3 = m_4 = 2m_c$ . The input parameters are  $\sqrt{s} = 10.6$  GeV,  $m_c = 1.5$  GeV,  $\alpha_s = 0.26$  (corresponding to  $\mu = 2m_c$  and  $\Lambda_{\overline{MS}}^{(4)} = 338$  MeV), and the wave functions at the origin are taken from a potential model calculation (see the QCD (BT(Buchmüller-Tye)) model in Ref.[20]):  $|R_{1S}(0)|^2 = 0.810\text{GeV}^3$ ,  $|R_{2S}(0)|^2 = 0.529\text{GeV}^3$ ,  $|R_{3S}(0)|^2 = 0.455\text{GeV}^3$ ,  $|R'_{1P}(0)|^2 = 0.075\text{GeV}^5$ ,  $|R'_{2P}(0)|^2 = 0.102\text{GeV}^5$ , and  $|R''_{1D}(0)|^2 = 0.015\text{GeV}^7$ .

### A. The $\psi(nS)\eta_c(mS)$ production

In the two S-wave (nS and mS) case, the cross section for  $e^+ + e^- \rightarrow \gamma^* \rightarrow H_1(nS) + H_2(mS)$  is given by

$$\sigma(e^+(p_1) + e^-(p_2) \rightarrow H_1(p_3) + H_2(p_4)) = \frac{2\pi\alpha^2\alpha_s^2|R_{ns}(0)|^2|R_{ms}(0)|^2\sqrt{s^2 - 2s(m_3^2 + m_4^2) + (m_3^2 - m_4^2)^2}}{81m_c^2s^2} \int_{-1}^1 |\bar{M}|^2 d\cos\theta, \quad (8)$$

where  $\theta$  is the scattering angle between  $\vec{p}_1$  and  $\vec{p}_3$ ,  $|\bar{M}|^2$  is as follows

$$|\bar{M}_{\eta_c\psi}|^2 = \frac{16384m_c^2(t^2 + u^2 - 32m_c^4)}{(8m_c^2 - t - u)^5}. \quad (9)$$

Here the Mandelstam variables are defined as

$$s = (p_1 + p_2)^2, \quad (10)$$

$$t = (p_3 - p_1)^2 = \frac{m_3^2 + m_4^2 - s}{2} + \frac{\sqrt{s^2 - 2s(m_3^2 + m_4^2) + (m_3^2 - m_4^2)^2}}{2} \cos\theta, \quad (11)$$

$$u = (p_3 - p_2)^2 = \frac{m_3^2 + m_4^2 - s}{2} - \frac{\sqrt{s^2 - 2s(m_3^2 + m_4^2) + (m_3^2 - m_4^2)^2}}{2} \cos\theta, \quad (12)$$

The cross sections for the double S-wave charmonium production are listed as follows

$$\sigma(e^+ + e^- \rightarrow J/\psi(1S) + \eta_c(1S)[\eta_c(2S), \eta_c(3S)]) = 5.5[3.6, 3.1] \text{ fb}, \quad (13)$$

$$\sigma(e^+ + e^- \rightarrow \psi(2S) + \eta_c(1S)[\eta_c(2S), \eta_c(3S)]) = 3.6[2.3, 2.0] \text{ fb}, \quad (14)$$

where the values in the brackets are the cross sections respectively for  $\eta_c(2S)$  and  $\eta_c(3S)$  with recoiling  $\psi$  mesons.

### B. The $\psi(nS)\chi_{cJ}(mP)(J = 0, 1, 2)$ production

In the one spin-triplet S-wave (nS) and one spin-triplet P-wave (mP) case, the cross section for  $e^+ + e^- \rightarrow \gamma^* \rightarrow H_1(nS) + H_2(mP)$  process reads

$$\sigma(e^+(p_1) + e^-(p_2) \rightarrow H_1(p_3) + H_2(p_4)) = \frac{2\pi\alpha^2\alpha_s^2|R_{ns}(0)|^2|R'_{mp}(0)|^2\sqrt{s^2 - 2s(m_3^2 + m_4^2) + (m_3^2 - m_4^2)^2}}{27m_c^2s^2} \int_{-1}^1 |\bar{M}|^2 d\cos\theta. \quad (15)$$

Here for the production of spin-triplet states  $\psi\chi_{cJ}$ ,  $|\bar{M}|^2$  is given in Eq. (16) for  $\chi_{c0}$ , in Eq. (17) for  $\chi_{c1}$  and Eq. (18) for  $\chi_{c2}$ ,

$$\begin{aligned} |\bar{M}_{\psi\chi_{c0}}|^2 = & 2048(90112m_c^{10} - 74752m_c^8t - 74752m_c^8u + 23360m_c^6t^2 + 43136m_c^6tu \\ & + 23360m_c^6u^2 - 3152m_c^4t^3 - 7600m_c^4t^2u - 7600m_c^4tu^2 - 3152m_c^4u^3 \\ & + 162m_c^2t^4 + 444m_c^2t^3u + 564m_c^2t^2u^2 + 444m_c^2tu^3 + 162m_c^2u^4 \\ & - t^4u - 3t^3u^2 - 3t^2u^3 - tu^4)/(3s^7m_c^2). \end{aligned} \quad (16)$$

$$\begin{aligned} |\bar{M}_{\psi\chi_{c1}}|^2 = & 32768(1792m_c^8 + 256m_c^6t + 256m_c^6u - 56m_c^4t^2 - 64m_c^4tu - 56m_c^4u^2 - 4m_c^2t^3 \\ & - 20m_c^2t^2u - 20m_c^2tu^2 - 4m_c^2u^3 + t^4 + 2t^3u + 2t^2u^2 + 2tu^3 + u^4)/s^7, \end{aligned} \quad (17)$$

$$\begin{aligned} |\bar{M}_{\psi\chi_{c2}}|^2 = & 4096(145408m_c^{10} - 1024m_c^8t - 1024m_c^8u - 2368m_c^6t^2 - 6400m_c^6tu - 2368m_c^6u^2 \\ & + 16m_c^4t^3 - 208m_c^4t^2u - 208m_c^4tu^2 + 16m_c^4u^3 + 24m_c^2t^4 + 72m_c^2t^3u + 96m_c^2t^2u^2 \\ & + 72m_c^2tu^3 + 24m_c^2u^4 - t^4u - 3t^3u^2 - 3t^2u^3 - tu^4)/(3s^7m_c^2). \end{aligned} \quad (18)$$

For the known spin-triplet P-wave states  $\chi_{cJ}(1P)(J = 0, 1, 2)$  we find

$$\sigma(e^+ + e^- \rightarrow J/\psi(1S) + \chi_{c0}(1P)[\chi_{c1}(1P), \chi_{c2}(1P)]) = 6.7[1.1, 1.6] \text{ fb}, \quad (19)$$

$$\sigma(e^+ + e^- \rightarrow \psi(2S) + \chi_{c0}(1P)[\chi_{c1}(1P), \chi_{c2}(1P)]) = 4.4[0.74, 1.1] \text{ fb}, \quad (20)$$

For the excited spin-triplet  $2P$  states  $\chi_{cJ}(2P)(J = 0, 1, 2)$ , which are to be searched for, we find

$$\sigma(e^+ + e^- \rightarrow J/\psi(1S) + \chi_{c0}(2P)[\chi_{c1}(2P), \chi_{c2}(2P)]) = 9.1[1.6, 2.2] \text{ fb}, \quad (21)$$

$$\sigma(e^+ + e^- \rightarrow \psi(2S) + \chi_{c0}(2P)[\chi_{c1}(2P), \chi_{c2}(2P)]) = 5.9[1.0, 1.4] \text{ fb}. \quad (22)$$

In Eqs. (19–22), we see that the cross sections for the excited  $2P$  states  $\chi_{cJ}(2P)$  are somewhat larger than that for the corresponding  $1P$  states  $\chi_{cJ}(1P)$  in the nonrelativistic limit. This numerical result is due to the fact that we have chosen the first derivative of the wave function at the origin for the  $2P$  states to be larger than that for the  $1P$  states, and actually the former could be slightly smaller than the latter, depending on the potentials that are used (see the values in the QCD (BT) model and other models in Ref.[20]). Furthermore, another important effect comes from the relativistic corrections, which may lower the cross sections for the  $\chi_{cJ}(2P)$  states. E.g., if we take the charm quark mass to be  $2m_c = M(2P) \approx 4 \text{ GeV}$  for the  $2P$  states, then the cross sections will be substantially lower. Despite of these uncertainties, we expect that the cross sections for the  $2P$  states should be comparable to that for the  $1P$  states.

### C. The $\eta_c(nS)h_c(mP)$ production

To search for the spin singlet P-wave charmonium  $h_c$  is certainly interesting. Recently, CLEO has found evidence for  $h_c$  in the  $\psi(2S) \rightarrow \pi^0 h_c$  decay followed by  $h_c \rightarrow \gamma \eta_c$  with a mass of  $M(h_c) = 3524.4 \pm 0.6 \pm 0.4 \text{ MeV}$  and hyperfine splitting of about 1.0 MeV measured in both the  $\eta_c$  exclusive and inclusive analysis[21]. It will also be interesting to search for the  $h_c$  in  $e^+e^-$  annihilation at  $\sqrt{s} = 10.6 \text{ GeV}$  in the recoil spectra of charge parity  $C=+1$  states such as  $\eta_c, \chi_{c0}, \chi_{c1}, \chi_{c2}$ . For the production of one spin-singlet S-wave state  $\eta_c(nS)$  and one spin-singlet P-wave state  $h_c(mP)$ , differing from [9], we find  $|\bar{M}|^2$  to be not vanishing but given by Eq. (23):

$$\begin{aligned} |\bar{M}_{\eta_c h_c}|^2 &= 2048(8192m_c^{10} + 1024m_c^8 t + 1024m_c^8 u + 320m_c^6 t^2 + 128m_c^6 t u + 320m_c^6 u^2 \\ &\quad - 16m_c^4 t^3 - 112m_c^4 t^2 u - 112m_c^4 t u^2 - 16m_c^4 u^3 + 2m_c^2 t^4 - 4m_c^2 t^3 u - 12m_c^2 t^2 u^2 \\ &\quad - 4m_c^2 t u^3 + 2m_c^2 u^4 - t^4 u - 3t^3 u^2 - 3t^2 u^3 - t u^4) / ((8m_c^2 - t - u)^7 m_c^2). \end{aligned} \quad (23)$$

For the spin-singlet P-wave states  $h_c(1P)$  and  $h_c(2P)$  we find

$$\sigma(e^+ + e^- \rightarrow \eta_c(1S) + h_c(1P)[h_c(2P)]) = 0.73[0.99] \text{ fb}, \quad (24)$$

$$\sigma(e^+ + e^- \rightarrow \eta_c(2S) + h_c(1P)[h_c(2P)]) = 0.48[0.65] \text{ fb}, \quad (25)$$

$$\sigma(e^+ + e^- \rightarrow \eta_c(3S) + h_c(1P)[h_c(2P)]) = 0.41[0.56] \text{ fb}. \quad (26)$$

#### D. The $\chi_{cJ}(nP)(J = 0, 1, 2)h_c(mP)$ production

In the two P-wave (nP and mP) case, the cross section for  $e^+ + e^- \rightarrow \gamma^* \rightarrow H_1(nP) + H_2(mP)$  is

$$\begin{aligned} \sigma(e^+(p_1) + e^-(p_2) \rightarrow H_1(p_3) + H_2(p_4)) = \\ \frac{2\pi\alpha^2\alpha_s^2|R'_p(0)|^4\sqrt{s^2 - 2s(m_3^2 + m_4^2) + (m_3^2 - m_4^2)^2}}{9m_c^2s^2} \int_{-1}^1 |\bar{M}|^2 d\cos\theta. \end{aligned} \quad (27)$$

For the  $\chi_{cJ}h_c$  production  $|\bar{M}|^2$  reads

$$|\bar{M}_{\chi_{c0}h_c}|^2 = 16384(t^2 + u^2 - 32m_c^4)(16m_c^2 - 3t - 3u)^2/(3(8m_c^2 - t - u)^7m_c^2), \quad (28)$$

$$\begin{aligned} |\bar{M}_{\chi_{c1}h_c}|^2 = & -4096(8192m_c^{10} - 3072m_c^8t - 3072m_c^8u + 2048m_c^6t^2 + 3584m_c^6tu \\ & + 2048m_c^6u^2 - 16m_c^4t^3 + 144m_c^4t^2u + 144m_c^4tu^2 - 16m_c^4u^3 - 52m_c^2t^4 \\ & - 128m_c^2t^3u - 152m_c^2t^2u^2 - 128m_c^2tu^3 - 52m_c^2u^4 + t^4u \\ & + 3t^3u^2 + 3t^2u^3 + tu^4)/((8m_c^2 - t - u)^7m_c^4), \end{aligned} \quad (29)$$

$$\begin{aligned} |\bar{M}_{\chi_{c2}h_c}|^2 = & -8192(544m_c^4 + 72m_c^2t + 72m_c^2u + 3t^2 + 6tu + 3u^2) \\ & \times (32m_c^4 - t^2 - u^2)/(3(8m_c^2 - t - u)^7m_c^2), \end{aligned} \quad (30)$$

and the corresponding cross sections are

$$\sigma(e^+ + e^- \rightarrow \chi_{c0}(1P) + h_c(1P)[h_c(2P)]) = 0.22[0.31] \text{ fb}, \quad (31)$$

$$\sigma(e^+ + e^- \rightarrow \chi_{c1}(1P) + h_c(1P)[h_c(2P)]) = 1.0[1.4] \text{ fb}, \quad (32)$$

$$\sigma(e^+ + e^- \rightarrow \chi_{c2}(1P) + h_c(1P)[h_c(2P)]) = 0.063[0.085] \text{ fb}. \quad (33)$$



**E. The  $\psi(nS)^1D_2(mP)$  production**

The cross section for  $e^+ + e^- \rightarrow \gamma^* \rightarrow H_1(nS) + H_2(mD)$  process is formulated as

$$\sigma(e^+(p_1) + e^-(p_2) \rightarrow H_1(p_3) + H_2(p_4)) = \frac{2\pi\alpha^2\alpha_s^2|R_S(0)|^2|R_D''(0)|^2\sqrt{s^2 - 2s(m_3^2 + m_4^2) + (m_3^2 - m_4^2)^2}}{27m_c^2s^2} \int_{-1}^1 |\bar{M}|^2 d\cos\theta, \quad (34)$$

$$|\bar{M}_{J/\psi^1D_2}| = -327680(16m_c^2 - s)^2(512m_c^6 - 32m_c^4s - 128m_c^4t - 128m_c^4u + 8m_c^2st + 8m_c^2su + 8m_c^2t^2 + 16m_c^2tu + 8m_c^2u^2 - st^2 - su^2)/(3m_c^2s^8), \quad (35)$$

and the numerical result is

$$\sigma(e^+ + e^- \rightarrow J/\psi(1S)[2s] + ^1D_2) = 0.19[0.12] \text{ fb.} \quad (36)$$

**F. The  $\chi_{cJ}(nP)(J = 0, 1, 2)^3D'_J(mD)(J' = 1, 2, 3)$  production**

The cross section for  $e^+ + e^- \rightarrow \gamma^* \rightarrow H_1(nP) + H_2(mD)$  process is formulated as

$$\sigma(e^+(p_1) + e^-(p_2) \rightarrow H_1(p_3) + H_2(p_4)) = \frac{2\pi\alpha^2\alpha_s^2|R_P(0)|^2|R_D''(0)|^2\sqrt{s^2 - 2s(m_3^2 + m_4^2) + (m_3^2 - m_4^2)^2}}{27m_c^2s^2} \int_{-1}^1 |\bar{M}|^2 d\cos\theta, \quad (37)$$

$$\begin{aligned} |\bar{M}_{\chi_{c1}^3D_1}| = & 20480(113393664m_c^{12} - 49483776m_c^{10}s - 28348416m_c^{10}t - 28348416m_c^{10}u \\ & + 7436288m_c^8s^2 + 12601344m_c^8st + 12601344m_c^8su + 1829376m_c^8t^2 \\ & + 3428352m_c^8tu + 1829376m_c^8u^2 - 413120m_c^6s^3 - 912960m_c^6st^2 \\ & - 1932032m_c^6s^2t - 1932032m_c^6s^2u - 1324416m_c^6stu - 912960m_c^6su^2 \\ & + 5600m_c^4s^4 + 114816m_c^4s^3t + 114816m_c^4s^3u + 165024m_c^4s^2t^2 + 152960m_c^4s^2tu \\ & + 165024m_c^4s^2u^2 + 144m_c^2s^5 - 2312m_c^2s^4t - 2312m_c^2s^4u - 12184m_c^2s^3t^2 \\ & - 4336m_c^2s^3tu - 12184m_c^2s^3u^2 + 289s^4t^2 + 289s^4u^2)/(5m_c^4s^9), \end{aligned} \quad (38)$$

$$\begin{aligned}
|\bar{M}_{\chi_{c1} \ 3D_2}| &= 2560(58589184m_c^{14} - 2293760m_c^{12}s - 14647296m_c^{12}t - 4286464m_c^{10}s^2 \\
&\quad - 14647296m_c^{12}u + 6922240m_c^{10}st + 6922240m_c^{10}su + 2502656m_c^{10}t^2 \\
&\quad - 1343488m_c^{10}tu + 2502656m_c^{10}u^2 + 576512m_c^8s^3 - 1119744m_c^8s^2t \\
&\quad - 938496m_c^8st^2 - 1119744m_c^8s^2u + 146432m_c^8stu - 938496m_c^8su^2 \\
&\quad + 4096m_c^6s^4 + 72192m_c^6s^3t - 1248m_c^4s^5 - 5984m_c^4s^3t^2 - 6080m_c^4s^3tu \\
&\quad + 72192m_c^6s^3u + 224m_c^2s^4t^2 + 119488m_c^6s^2t^2 + 40960m_c^6s^2tu \\
&\quad - 1792m_c^4s^4t + 119488m_c^6s^2u^2 - 1792m_c^4s^4u - 5984m_c^4s^3u^2 \\
&\quad - 48m_c^2s^6 + 224m_c^2s^4u^2 + 3s^7 - 3s^5t^2 + 6s^5tu - 3s^5u^2)/(m_c^6s^9), \tag{39}
\end{aligned}$$

$$\begin{aligned}
|\bar{M}_{\chi_{c1} \ 3D_3}| &= 40960(7446528m_c^{10} - 756224m_c^8s - 1861632m_c^8t + 393856m_c^6st \\
&\quad - 1861632m_c^8u - 62208m_c^6s^2 + 393856m_c^6su + 167552m_c^6t^2 + 130304m_c^6tu \\
&\quad + 167552m_c^6u^2 + 9632m_c^4s^3 - 27968m_c^4s^2t - 27968m_c^4s^2u - 39568m_c^4st^2 \\
&\quad - 19328m_c^4stu - 39568m_c^4su^2 - 288m_c^2s^4 + 664m_c^2s^3t + 664m_c^2s^3u \\
&\quad + 752m_c^2s^2tu + 3120m_c^2s^2t^2 + 3120m_c^2s^2u^2 - 83s^3t^2 \\
&\quad - 83s^3u^2)(16m_c^2 - s)/(5m_c^4s^9), \tag{40}
\end{aligned}$$

$$\begin{aligned}
|\bar{M}_{\chi_{c2} \ 3D_1}| &= 640(29807345664m_c^{14} - 6599344128m_c^{12}s - 7451836416m_c^{12}t \\
&\quad - 7451836416m_c^{12}u + 182222848m_c^{10}s^2 + 2217541632m_c^{10}st + 2217541632m_c^{10}su \\
&\quad + 647626752m_c^{10}tu + 607666176m_c^{10}t^2 + 607666176m_c^{10}u^2 + 43309056m_c^8s^3 \\
&\quad - 233439232m_c^8s^2t - 233439232m_c^8s^2u - 205805568m_c^8st^2 - 142774272m_c^8stu \\
&\quad - 205805568m_c^8su^2 - 3057664m_c^6s^4 + 10221568m_c^6s^3t + 10221568m_c^6s^3u \\
&\quad + 24313856m_c^6s^2t^2 + 9732096m_c^6s^2tu + 24313856m_c^6s^2u^2 + 66368m_c^4s^5 \\
&\quad - 163072m_c^4s^4t - 163072m_c^4s^4u - 1174848m_c^4s^3t^2 - 400m_c^2s^6 \\
&\quad - 205696m_c^4s^3tu - 1174848m_c^4s^3u^2 + 20768m_c^2s^4t^2 \\
&\quad - 768m_c^2s^4tu + 20768m_c^2s^4u^2 + s^7 - s^5t^2 + 2s^5tu - s^5u^2)/(15m_c^6s^9), \tag{41}
\end{aligned}$$

$$\begin{aligned}
|\bar{M}_{\chi_{c2} \ ^3D_2}| &= 81920(13979648m_c^{12} - 1540096m_c^{10}s - 3494912m_c^{10}t - 3494912m_c^{10}u \\
&\quad - 62400m_c^8s^2 + 724224m_c^8st + 724224m_c^8su + 303232m_c^8t^2 + 267264m_c^8tu \\
&\quad + 303232m_c^8u^2 + 14208m_c^6s^3 - 55440m_c^6s^2t - 55440m_c^6s^2u - 71376m_c^6st^2 \\
&\quad - 38304m_c^6stu - 71376m_c^6su^2 - 624m_c^4s^4 + 1872m_c^4s^3t + 1872m_c^4s^3u \\
&\quad + 6018m_c^4s^2t^2 + 1824m_c^4s^2tu + 6018m_c^4s^2u^2 + 9m_c^2s^5 - 24m_c^2s^4t \\
&\quad - 24m_c^2s^4u - 219m_c^2s^3t^2 - 30m_c^2s^3tu - 219m_c^2s^3u^2 \\
&\quad + 3s^4t^2 + 3s^4u^2)/(m_c^4s^9), \tag{42}
\end{aligned}$$

$$\begin{aligned}
|\bar{M}_{\chi_{c2} \ ^3D_3}| &= 5120(883687424m_c^{14} - 77856768m_c^{12}s - 220921856m_c^{12}t \\
&\quad - 220921856m_c^{12}u - 2650112m_c^{10}s^2 + 40353792m_c^{10}st + 40353792m_c^{10}su \\
&\quad + 19030016m_c^{10}t^2 + 17170432m_c^{10}tu + 19030016m_c^{10}u^2 + 1043456m_c^8s^3 \\
&\quad - 2798592m_c^8s^2t - 2798592m_c^8s^2u - 3923968m_c^8st^2 - 2240512m_c^8stu \\
&\quad - 3923968m_c^8su^2 - 95744m_c^6s^4 + 89088m_c^6s^3t + 89088m_c^6s^3u \\
&\quad + 332416m_c^6s^2t^2 + 34816m_c^6s^2tu + 332416m_c^6s^2u^2 + 3968m_c^4s^5 \\
&\quad - 1152m_c^4s^4t - 1152m_c^4s^4u - 12928m_c^4s^3t^2 + 3584m_c^4s^3tu \\
&\quad - 12928m_c^4s^3u^2 - 80m_c^2s^6 + 208m_c^2s^4t^2 - 128m_c^2s^4tu + 208m_c^2s^4u^2 \\
&\quad + s^7 - s^5t^2 + 2s^5tu - s^5u^2)/(5m_c^6s^9). \tag{43}
\end{aligned}$$

The numerical results are listed as follows, where  $\delta_1 \equiv ^3D_1$ ,  $\delta_2 \equiv ^3D_2$ ,  $\delta_3 \equiv ^3D_3$ ,

$$\sigma(e^+ + e^- \rightarrow \chi_{c1}[\chi_{c2}] + \delta_1) = 0.080[0.041] \text{ fb}, \tag{44}$$

$$\sigma(e^+ + e^- \rightarrow \chi_{c1}[\chi_{c2}] + \delta_2) = 0.099[0.084] \text{ fb}, \tag{45}$$

$$\sigma(e^+ + e^- \rightarrow \chi_{c1}[\chi_{c2}] + \delta_3) = 0.041[0.0099] \text{ fb}, \tag{46}$$

As a summary of the above results, we show the differential cross sections (the angular distribution functions) for different double charmonium production processes at leading order in NRQCD (QED contributions are not included) in Table I, and the corresponding graphs in Fig. 1-7.

### III. QED PROCESSES INCLUDING $J^{PC} = 1^{--}$ STATES

Since the  $J^{PC} = 1^{--}$   $c\bar{c}$  can be produced via a single photon, the QED contribution may be significant or even comparable to the QCD contribution in some exclusive processes involving one  $J^{PC\mathcal{G}} = 1^{--}$  charmonium state. These QED effects are considered in [9, 22]. There are six Feynman diagrams for the QED process at  $\alpha^4$  order, and only two represent  $\gamma^* \rightarrow c\bar{c}\gamma^* \rightarrow (c\bar{c})_{1^{--}}c\bar{c}$ , which is dominant and has been calculated in [9, 22]. In this paper we include all the eight diagrams to get the full result at order  $\alpha^4$ , though the contributions of other six diagrams are numerically small. Using the notation in section II, we re-express below the analytical formulas of the exclusive processes including both QCD and QED contributions.

#### A. The $\psi(nS)\eta_c(mS)$ production

The cross section for  $e^+ + e^- \rightarrow \gamma^* \rightarrow H_1(nS) + H_2(mS)$  is now changed to

$$\sigma(e^+(p_1) + e^-(p_2) \rightarrow H_1(p_3) + H_2(p_4)) = \frac{\alpha^2 |R_{ns}(0)|^2 |R_{ms}(0)|^2 \sqrt{s^2 - 2s(m_3^2 + m_4^2) + (m_3^2 - m_4^2)^2}}{288m_c^2\pi s^2} \int_{-1}^1 |\bar{M}|^2 dx, \quad (47)$$

where  $x = \cos\theta$  and  $\theta$  is the scattering angle between  $\vec{p}_1$  and  $\vec{p}_3$ . And  $|\bar{M}|^2$  is

$$|\bar{M}|^2 = \frac{2048(s - 16m_c^2)(16\alpha m_c^2 + 48\alpha_s m c^2 + 3\alpha s)^2}{81m_c^2 s^4} \quad (48)$$

The numerical results become

$$\sigma(e^+ + e^- \rightarrow J/\psi(1S) + \eta_c(1S)[\eta_c(2S), \eta_c(3S)]) = 6.6[4.3, 3.7] \text{ fb}, \quad (49)$$

$$\sigma(e^+ + e^- \rightarrow \psi(2S) + \eta_c(1S)[\eta_c(2S), \eta_c(3S)]) = 4.3[2.8, 2.4] \text{ fb}, \quad (50)$$

where the values in the brackets are the cross sections respectively for  $\eta_c(2S)$  and  $\eta_c(3S)$  with recoiled  $\psi$  mesons.

## B. The $\psi(ns) + \chi_{cJ}(mp)$ Production

The cross section for  $e^+ + e^- \rightarrow \gamma^* \rightarrow H_1(nS) + H_2(mS)$  is changed to

$$\sigma(e^+(p_1) + e^-(p_2) \rightarrow H_1(p_3) + H_2(p_4)) = \frac{\alpha^2 |R_{ns}(0)|^2 |R'_{mp}(0)|^2 \sqrt{s^2 - 2s(m_3^2 + m_4^2)} + (m_3^2 - m_4^2)^2}{96m_c^2 \pi s^2} \int_{-1}^1 |\bar{M}|^2 dx. \quad (51)$$

And now  $|\bar{M}|^2$  for  $\psi\chi_{c0}, \psi\chi_{c1}, \psi\chi_{c2}$  production, are given in Eq. (52), Eq. (53), Eq. (54) respectively.

$$\begin{aligned} |\bar{M}_{\psi\chi_{c0}}|^2 &= (2048\pi^2((589824(x^2 - 1)m_c^{10} - 4096s(73x^2 + 25)m_c^8 - 2048s^2(x^2 - 1)m_c^6 \\ &+ 128s^3(25x^2 + 17)m_c^4 + 16s^4(x^2 - 1)m_c^2 - 9s^5(x^2 + 1))\alpha^2 \\ &+ 48\alpha_s m_c^2(73728(x^2 - 1)m_c^8 - 3584s(13x^2 + 1)m_c^6 + 64s^2(71x^2 + 55)m_c^4 \\ &+ 56s^3(5x^2 + 1)m_c^2 - s^4(25x^2 + 29))\alpha + 144\alpha_s^2 m_c^2(36864(x^2 - 1)m_c^8 \\ &- 256s(109x^2 - 11)m_c^6 + 128s^2(41x^2 + 22)m_c^4 - 4s^3(61x^2 + 101)m_c^2 \\ &+ s^4(x^2 - 1))))/(243m_c^4 s^6). \end{aligned} \quad (52)$$

$$\begin{aligned} |\bar{M}_{\psi\chi_{c1}}|^2 &= (4096\pi(192\alpha\alpha_s(9216(x^2 - 1)m_c^6 - 64s(31x^2 + 19)m_c^4 + 8s^2(9x^2 - 19)m_c^2 \\ &+ s^3(x^2 + 25))m_c^4 + 2304\alpha_s^2(1152(x^2 - 1)m_c^6 - 8s(49x^2 + 1)m_c^4 \\ &+ 4s^2(9x^2 + 5)m_c^2 - s^3(x^2 + 1))m_c^4 + \alpha^2(294912(x^2 - 1)m_c^{10} \\ &- 2048s(13x^2 + 37)m_c^8 - 19456s^2 m_c^6 + 32s^3(x^2 - 23)m_c^4 + 144s^4 x^2 m_c^2 \\ &- 9s^5(x^2 + 1))))/(81m_c^4 s^6). \end{aligned} \quad (53)$$

$$\begin{aligned} |\bar{M}_{\psi\chi_{c2}}|^2 &= (4096\pi^2((1474560(x^2 - 1)m_c^{10} + 2048s(31x^2 - 233)m_c^8 - 1024s^2(32x^2 + 1)m_c^6 \\ &- 32s^3(35x^2 - 101)m_c^4 + 16s^4(19x^2 - 10) - 9s^5(x^2 + 1))\alpha^2 \\ &+ 48\alpha_s m_c^2(184320(x^2 - 1)m_c^8 - 256s(59x^2 + 143)m_c^6 - 32s^2(59x^2 - 89)m_c^4 \\ &+ 4s^3(61x^2 + 29)m_c^2 - s^4(7x^2 + 11))\alpha + 144\alpha_s^2 m_c^2(92160(x^2 - 1)m_c^8 \\ &- 128s(149x^2 + 53)m_c^6 + 64s^2(25x^2 + 23)m_c^4 - 32s^3(2x^2 + 1)m_c^2 \\ &+ s^4(x^2 - 1))))/(243m_c^4 s^6). \end{aligned} \quad (54)$$

The numerical results of spin-triplet P-wave states  $\chi_{cJ}(1P)$  ( $J = 0, 1, 2$ ) are

$$\sigma(e^+ + e^- \rightarrow J/\psi(1S) + \chi_{c0}(1P)[\chi_{c1}(1P), \chi_{c2}(1P)]) = 6.9[1.0, 1.8] \text{ fb}, \quad (55)$$

$$\sigma(e^+ + e^- \rightarrow \psi(2S) + \chi_{c0}(1P)[\chi_{c1}(1P), \chi_{c2}(1P)]) = 4.5[0.7, 1.1] \text{ fb}, \quad (56)$$

And for the excited spin-triplet 2P states  $\chi_{cJ}(2P)(J = 0, 1, 2)$ , the results turn to be

$$\sigma(e^+ + e^- \rightarrow J/\psi(1S) + \chi_{c0}(2P)[\chi_{c1}(2P), \chi_{c2}(2P)]) = 9.4[1.4, 2.4] \text{ fb}, \quad (57)$$

$$\sigma(e^+ + e^- \rightarrow \psi(2S) + \chi_{c0}(2P)[\chi_{c1}(2P), \chi_{c2}(2P)]) = 6.2[0.9, 1.6] \text{ fb}. \quad (58)$$

### C. The $\psi(ns) + 1D2$ Production

The cross section for  $e^+ + e^- \rightarrow \gamma^* \rightarrow H_1(nS) + H_2(mD)$  process is

$$\begin{aligned} \sigma(e^+(p_1) + e^-(p_2) \rightarrow H_1(p_3) + H_2(p_4)) = \\ \frac{5\alpha^2 |R_S(0)|^2 |R_D''(0)|^2 \sqrt{s^2 - 2s(m_3^2 + m_4^2) + (m_3^2 - m_4^2)^2}}{192m_c^2 \pi s^2} \int_{-1}^1 |\bar{M}|^2 dx, \end{aligned} \quad (59)$$

and

$$|\bar{M}_{J/\psi 1D_2}|^2 = \frac{4096\pi^2 (s - 16m_c^2)^3 (32\alpha m_c^2 + 96\alpha_s m_c^2 + 3s\alpha)^2 (x^2 + 1)}{243m_c^6 s^6}, \quad (60)$$

and the numerical result becomes

$$\sigma(e^+ + e^- \rightarrow J/\psi(1S)[2s] + {}^1D_2) = 0.21[0.13] \text{ fb}. \quad (61)$$

### D. The $\eta_c(ns) + \psi_{3D1}$ Production

The cross section for  $e^+ + e^- \rightarrow \gamma^* \rightarrow H_1(nS) + H_2(mD)$  process is formulated as

$$\begin{aligned} \sigma(e^+(p_1) + e^-(p_2) \rightarrow H_1(p_3) + H_2(p_4)) = \\ \frac{5\alpha^2 |R_S(0)|^2 |R_D''(0)|^2 \sqrt{s^2 - 2s(m_3^2 + m_4^2) + (m_3^2 - m_4^2)^2}}{192m_c^2 \pi s^2} \int_{-1}^1 |\bar{M}|^2 dx, \end{aligned} \quad (62)$$

and

$$\begin{aligned} |\bar{M}_{\eta_c \ 3D_1}|^2 = 512\pi^2 (s - 16m_c^2) (48\alpha_s (64m_c^2 - 9s)m_c^2 + \alpha(1024m_c^4 - 144sm_c^2 - 15s^2))^2 \\ (x^2 + 1) / (1215m_c^6 s^6), \end{aligned} \quad (63)$$

and the numerical result becomes

$$\sigma(e^+ + e^- \rightarrow \eta_c(1S) + {}^3D_1) = 0.17 \text{ fb}. \quad (64)$$

## E. conclusion

In this section we have considered the QED contribution to the exclusive processes involving one  $J^{pc} = 1^{--}$  charmonium state (e.g.,  $\psi(nS)$  and  $\psi_{3D1}$ ). We find that in general by adding QED contribution the cross section can be changed by the order of ten percent. We list the results below with  $\sqrt{s} = 10.6\text{GeV}$ ,  $\alpha_s = 0.26$ ,  $m_c = 1.5\text{GeV}$ . The cross sections of  $\psi(ns) + \eta_c(ms)$  are increased by 20 percent, that of  $\psi(ns) + \chi_{cJ}$  are increased by 4, -5, 8 percent for  $J = 0, 1, 2$  respectively, that of  $\psi(ns) + {}^1D_2$  is increased by 11 percent, and that of  $\eta_c(ns) + {}^3D_1$  is increased by 9 percent. In [9] the authors also considered the QED process but only the two dominant diagrams were included. Our results are in agreement with their results in most processes when we choose the same parameters as theirs, except for the process of  $\eta_c + \psi({}^3D_1)$  production, for which they obtained 41% enhancement with QED effects whereas we get 19% with the same parameters. Here our analytical expression also differs from theirs.

We show the differential cross sections (the angular distribution functions) for different double charmonium production processes including both QCD and QED contributions in Table II, and the corresponding graphs in Fig. 8. Ratios of production cross sections of various double charmonia to that of  $J/\psi + \eta_c$  in  $e^+e^-$  annihilation at  $\sqrt{s} = 10.6$  GeV are listed in Table III.

## IV. DISCUSSION AND SUMMARY

In this paper, we make predictions for various double charmonia production processes in  $e^+e^-$  annihilation at  $\sqrt{s} = 10.6$  GeV with  $B$  factories, based on a complete leading order calculation including both QCD and QED contributions. In particular, we aim at searching for excited charmonium states in these processes. From the obtained results we make the following observations:

The calculated relative production rates for  $e^+e^- \rightarrow \psi(2S)\eta_c, \psi(2S)\chi_{c0}, \psi(2S)\eta_c(2S)$  are roughly compatible with the new Belle measurements [8] (see also [9]), assuming the decay branching ratios into charged tracks are comparable for  $\eta_c, \eta_c(2S)$ , and  $\chi_{c0}$ .

The calculated relative production rates for  $e^+e^- \rightarrow J/\psi\chi_{c0}(2P), J/\psi\eta_c(3S)$  and  $e^+e^- \rightarrow \psi(2S)\chi_{c0}(2P), \psi(2S)\eta_c(3S)$  are large, and these two states may be observable in the mass

range  $m_{2P} = 3.90 - 4.00$  GeV and  $m_{3S} = 3.95 - 4.10$  GeV respectively (see, e.g. [6]). Both of them are above the OZI (Okubo-Zweig-Iizuka) allowed thresholds, but unlike the  $\chi_{c0}(2P)$ , the  $\eta_c(3S)$  can not decay to  $D\bar{D}$  pair, which may distinguish between these two states experimentally.

The calculated relative production rate for  $e^+e^- \rightarrow h_c\eta_c$  is not zero. This differs from the result given in [9], but agrees with [22]. Hence the  $h_c$  might be observable via this channel with high statistics in the future. Aside from this process,  $e^+e^- \rightarrow h_c\chi_{c1}$  is also very hopeful in finding the  $h_c$  meson, since the  $\chi_{c1}$  has a large branching ratio (larger than 30%) decaying into  $\gamma J/\psi$ , and the  $J/\psi$  can be easily detected by the  $\mu^+\mu^-$  signal. Moreover, the calculated cross section for  $e^+e^- \rightarrow h_c\chi_{c1}$  is about 1.0 fb, not very small and much larger than that for  $h_c\chi_{c0}$  and  $h_c\chi_{c2}$  production rates.

We show the differential cross sections (the angular distribution functions) for different double charmonium production processes in Table I (not including QED contribution) and Table II (including both QCD and QED contributions), and the corresponding graphs in Fig. 1-7, and Fig. 8.

As a whole, our results agree with those in [9] and [22] (also agree with our previous result for  $J/\psi\eta_c(\chi_{c0}, \chi_{c1}, \chi_{c2})$ [10]), if using the same parameters. For the QED part, in [9, 22] only two dominant diagrams are taken into account, while in this paper all diagrams are considered, but the numerical contributions of the remaining four diagrams are small. However, there still exists a difference in the result for the  $e^+e^- \rightarrow \eta_c + \psi(^3D_1)$  production. As for numerical results, since we use a larger value of the strong coupling constant  $\alpha_s = 0.26$  (corresponding to  $\mu = 2m_c = 3.0$  GeV and  $\Lambda_{\overline{MS}}^{(4)} = 338$  MeV) than that in [9, 22], our predicted cross sections are in general larger than that in [9, 22]. Moreover, we use the charmonium wave functions and their derivatives at the origin (including the ground state and excited states) from the BT potential model calculation[20] but not from the experimental values of leptonic decay widths, etc., as in [9, 22], and this may further enlarge our predicted cross sections. These parameters may not be the best choice, but, at present, since we do not have enough available data for higher excited charmonium states, using the potential model calculation may still be a reasonable and tentative choice. We view these as theoretical uncertainties in our approach for the leading order calculations.

As emphasized above, this paper aims at searching for excited charmonium states in  $e^+e^-$  annihilation at  $\sqrt{s} = 10.6$  GeV with  $B$  factories. After the main part of the results were



presented in [23] (with a more complete leading order calculation including both QCD and QED contributions for various double charmonium production processes being added in its present form), a number of new experimental and theoretical results have appeared recently.

1. The double charmonium production in  $e^+e^-$  annihilation at B factories has been confirmed by the BaBar Collaboration (see Ref.[24]) with comparable cross sections to that observed by Belle. Theoretically, the large gap between experiment and theory could be largely narrowed by the next to leading order QCD radiative corrections [25] and relativistic corrections (see, Refs.[26, 27] and references therein) in the framework of nonrelativistic QCD, and other possible approaches (see, e.g.[28]).

2. Belle has observed the X(3940), a new charmonium state or charmonium-like state, in  $e^+e^- \rightarrow J/\psi X(3940)$  with  $M_X = (3.940 \pm 0.012) \text{ GeV}$ [29]. While its main decay mode is  $X(3940) \rightarrow D\bar{D}^*$ , no signal is found for  $X(3940) \rightarrow D\bar{D}$ . This rules out the possibility of X(3940) being the  $\chi_{c0}(2P)$  state. Furthermore, the X(3940) is unlikely to be the  $\chi_{c1}(2P)$  state, since no signal for the  $\chi_{c1}(1P)$  is found. This is in line with our calculation, which shows that the cross section for  $e^+e^- \rightarrow J/\psi\chi_{c1}(1P)$  is much smaller than  $e^+e^- \rightarrow J/\psi\eta_c$ . Finally, the X(3940) could be the  $\eta_c(3S)$  state. According to our calculation (see Eq.(13)), the production cross sections for  $\eta_c(1S)$ ,  $\eta_c(2S)$ ,  $\eta_c(3S)$  are respectively 5.5, 3.6, 3.1 fb, and the relative rates are roughly consistent with the signal yields  $N = 235 \pm 26$ ,  $164 \pm 30$ ,  $149 \pm 33$  events for  $\eta_c(1S)$ ,  $\eta_c(2S)$ , X(3940)[29]. This might be viewed as a support to interpreting the X(3940) as the  $\eta_c(3S)$ . However, the remaining problem is how to understand its low mass of X(3940) if it is the  $\eta_c(3S)$ , which is lower than potential model predictions by 50-120 MeV. But this could be explained by the coupled channel effects that the coupling of  $\eta_c(3S)$  to the  $0^+$  and  $0^-$  charmed meson pair (in S-wave) will lower the mass of  $\eta_c(3S)$ [30].

3. Belle has not observed the X(3872) in  $e^+e^- \rightarrow J/\psi X(3872)$ . This implies that the X(3872) is unlikely to be a conventional  $0^{-+}$  or  $0^{++}$  charmonium, since in our calculation they may have relatively large rates to be observed in double charmonium production. On the other hand, a  $1^{++}$  or  $2^{-+}$  charmonium could be possible for X(3872), since they have relatively small production rates. Of course, the nature of X(3872) needs clarifying by other more relevant experiments (see, e.g. [5]), aside from the  $e^+e^-$  annihilation processes.

4. Belle has very recently observed a new state, the X(4160), in the process of double charm production  $e^+e^- \rightarrow J/\psi + X(4160)$  followed by  $X(4160) \rightarrow D^*\bar{D}^*$ [31]. Possible interpretations for the X(4160) are discussed in[32] with emphasized possible assignments

of  $2^1D_2, \eta_c(4S), \chi_{c0}(3P)$  charmonium states and related problems.

In conclusion, we find that the double charmonium production processes in  $e^+e^-$  annihilation at  $B$  factories are very useful tools in searching for excited charmonium states or charmonium-like states. The leading order NRQCD calculation might hopefully provide a useful guide for the relative production rates, but not the absolute rates themselves. A systematical study for the QCD radiative corrections and relativistic corrections for different processes are apparently needed. On the other hand, studies of charmonium spectroscopy including charmonium masses, decays, and coupled channel effects, and the new type charmonium-like states are also very desirable.

### Acknowledgments

We thank P. Pakhlov for discussions on the Belle data and possible implications, and E. Braaten and J. Lee for communications on some calculations. This work was supported in part by the National Natural Science Foundation of China (No. 10421503, No. 10675003), the Key Grant Project of Chinese Ministry of Education (No. 305001), and the Research Found for Doctorial Program of Higher Education of China.

- 
- [1] T. Skwarnicki, *Int.J.Mod.Phys.* **A19**, 1030(2004), hep-ph/0311243.
  - [2] S.L. Olsen, *Int.J.Mod.Phys.* **A20**, 240(2005), hep-ex/0407033.
  - [3] C. Quigg, hep-ph/0403187; *Nucl.Phys.Proc.Suppl.* **142**, 87(2005).
  - [4] F.E. Close and P.R. Page, *Phys.Lett.* **B578**, 119(2004), hep-ph/0309253.
  - [5] E. Swanson, hep-ph/0601110.
  - [6] S. Godfrey, N. Isgur, *Phys. Rev.* **D32**, 189 (1985).
  - [7] Belle Collaboration, K. Abe *et al.*, *Phys. Rev. Lett.* **89**, 142001 (2002).
  - [8] Belle Collaboration, K. Abe *et al.*, hep-ex/0407009, *Phys. Rev. D* **70**, 071102 (2004).
  - [9] E. Braaten and J. Lee, *Phys. Rev.* **D67**, 054007 (2003).
  - [10] K.Y. Liu, Z.G. He and K.T. Chao, *Phys. Lett.* **B557**, 45 (2003).
  - [11] K. Hagiwara, E. Kou, C.-F. Qiao, *Phys. Lett.* **B570**, 39 (2003).

- [12] G. T. Bodwin, J. Lee, E. Braaten, Phys. Rev. **D67**, 054023 (2003); Phys. Rev. Lett. **90**, 162001 (2003);  
A. B. Kaidalov, JETP Lett. **77**, 349 (2003), Pisma Zh. Eksp. Teor. Fiz. **77**, 417 (2003), hep-ph/0301246;  
A. V. Berezhnoy, A. K. Likhoded, Phys. Atom. Nucl. **67**, 757(2004) ; Yad.Fiz. **67**, 778(2004), hep-ph/0303145;  
K.-Y. Liu, Z.-G. He, K.-T. Chao, Phys. Rev. **D68**, 031501(R) (2003);  
A. V. Luchinsky, Phys. Atom. Nucl. **68**, 1400(2005); Yad. Fiz. **68**, 1456(2005), hep-ph/0305253;  
S. J. Brodsky, A. S. Goldhaber, J. Lee, Phys. Rev. Lett. **91**, 112001 (2003);  
B. L. Ioffe, D. E. Kharzeev, Phys. Rev. **D69**, 014016(2004), hep-ph/0306062;  
S. Fleming, A. K. Leibovich, T. Mehen, Phys. Rev. **D68**, 094011(2003) , hep-ph/0306139;  
C.-F. Qiao, J.-X. Wang, Phys. Rev. **D69**, 014015(2004), hep-ph/0308244;  
S. Dulat, K. Hagiwara and Z.H. Lin, Phys. Lett. **B594**, 118(2004), hep-ph/0402230;  
K. Cheung and W.Y. Keung, Phys. Rev. **D69**, 094026 (2004).  
J.P. Ma and Z.G. Si, Phys. Rev. **D70**, 074007 (2004), hep-ph/0405111.
- [13] P. Cho and A.K. Leibovich, Phys. Rev. **D 54**, 6690 (1996).
- [14] F. Yuan, C.F. Qiao, and K.T. Chao, Phys. Rev. **D 56**, 321 (1997); Phys. Rev. **D 56**, 1663 (1997).
- [15] S. Baek, P. Ko, J. Lee, and H.S. Song, J. Korean Phys. Soc. **33**, 97 (1998).
- [16] K.Y. Liu, Z.G. He, and K.T. Chao, Phys. Rev. **D69**, 094027 (2004).
- [17] G.T. Bodwin, E. Braaten, and G.P. Lepage, Phys. Rev. **D51**, 1125 (1995).
- [18] P. Cho and A.K. Leibovich, Phys. Rev. **D53**, 150 (1996); **53**, 6203 (1996); P. Ko, J. Lee and H.S. Song, Phys. Rev. **D54**, 4312(1996); *ibid* **D60**, 119902(1999).
- [19] J.H. Kühn, J. Kaolan and E.G.O. Safiani, Nucl. Phys. **B157**, 125 (1979); B. Guberina, J.H. Kühn, R.D. Peccei and R. Rückl, Nucl. Phys. **B174**, 317(1980).
- [20] E.J. Eichten and C. Quigg, Phys. Rev. **D52**, 1726 (1995).
- [21] P. Rubin et al.(CLEO Collaboration), Phys.Rev. **D72**, 092004(2005), hep-ex/0508037.
- [22] E. Braaten and J. Lee, Phys. Rev. **D72**, 099901(E) (2005).
- [23] K.Y.Liu, Z.G.He and K.T.Chao, arxiv:hep-ph/0408141v2.
- [24] B. Aubert *et al*, The BABAR Collaboration, Phys.Rev. **D72**, 031101(2005).

- [25] Y.J. Zhang, Y.J. Gao and K.T. Chao, Phys. Rev. Lett. 96, 092001(2006); see also Y.J. Zhang and K.T. Chao, Phys. Rev. Lett.98, 092003 (2007).
- [26] G.T. Bodwin, D. Kang and J. Lee, Phys. Rev.**D74**, 014014 (2006)(hep-ph/0603186); hep-ph/0603185; G.T. Bodwin, D. Kang, D. Kim, J. Lee, and C. Yu, hep-ph/0611002.
- [27] Z.G. He, Y. Fan, and K.T. Chao, Phys. Rev. D75, 074011 (2007).
- [28] J.P. Ma and Z.G. Si, arXiv:hep-ph/0608221; V.V. Braguta, A.K. Likhoded, and A.V. Luchinsky, Phys. Rev. D72, 074019 (2005); arXiv:hep-ph/0602047; arXiv:hep-ph/0611021; A.E. Bondar and V.L. Chernyak, Phys. Lett. B612, 215 (2005); D. Ebert and A.P. Martynenko, Phys. Rev. D74, 054008 (2006); H.-M. Choi and C.-R. Ji, arXiv: 0707.1173 [hep-ph].
- [29] P. Pakhlov (Belle Collaboration), hep-ex/0412041.
- [30] E. Eichten, K. Lane, and C. Quigg, Phys. Rev. D73, 014014 (2006); 73, 079903(E)(2006).
- [31] I. Adachi et al. (Belle Collaboration), arXiv:0708.3812 [hep-ex].
- [32] K.T. Chao, arXiv:0707.3982[hep-ph].

TABLE I: Differential cross sections–angular distribution functions for double charmonium production in  $e^+e^-$  annihilation at  $\sqrt{s} = 10.6$  GeV (QED contributions not included; see text for the input parameters).

Differential cross section	Angular distribution function (fb)
$d\sigma(e^+ + e^- \rightarrow J/\psi + \eta_c(1S))/d\cos\theta$	$2.06(1 + \cos^2\theta)$
$d\sigma(e^+ + e^- \rightarrow J/\psi + \eta_c(2S))/d\cos\theta$	$1.34(1 + \cos^2\theta)$
$d\sigma(e^+ + e^- \rightarrow J/\psi + \eta_c(3S))/d\cos\theta$	$1.16(1 + \cos^2\theta)$
$d\sigma(e^+ + e^- \rightarrow J/\psi + \chi_{c0})/d\cos\theta$	$3.09(1 + 0.252\cos^2\theta)$
$d\sigma(e^+ + e^- \rightarrow J/\psi + \chi_{c1})/d\cos\theta$	$0.457(1 + 0.698\cos^2\theta)$
$d\sigma(e^+ + e^- \rightarrow J/\psi + \chi_{c2})/d\cos\theta$	$0.870(1 - 0.198\cos^2\theta)$
$d\sigma(e^+ + e^- \rightarrow \eta_c + hc(1p))/d\cos\theta$	$0.480(1 - 0.726\cos^2\theta)$
$d\sigma(e^+ + e^- \rightarrow \eta_c + hc(2p))/d\cos\theta$	$0.653(1 - 0.726\cos^2\theta)$
$d\sigma(e^+ + e^- \rightarrow \chi_{c1} + hc(1p))/d\cos\theta$	$0.483(1 + 0.190\cos^2\theta)$
$d\sigma(e^+ + e^- \rightarrow \chi_{c1} + hc(2p))/d\cos\theta$	$0.657(1 + 0.190\cos^2\theta)$
$d\sigma(e^+ + e^- \rightarrow \chi_{c2} + hc(1p))/d\cos\theta$	$0.0235(1 + \cos^2\theta)$
$d\sigma(e^+ + e^- \rightarrow \chi_{c2} + hc(2p))/d\cos\theta$	$0.0306(1 + \cos^2\theta)$
$\sigma(e^+ + e^- \rightarrow J/\psi(1S) + {}^1D_2)/d\cos\theta$	$0.0694(1 + \cos^2\theta)$
$d\sigma(e^+ + e^- \rightarrow \chi_{c1} + \delta_1)/d\cos\theta$	$0.0307(1 + 0.922\cos^2\theta)$
$d\sigma(e^+ + e^- \rightarrow \chi_{c1} + \delta_2)/d\cos\theta$	$0.0545(1 - 0.273\cos^2\theta)$
$d\sigma(e^+ + e^- \rightarrow \chi_{c1} + \delta_3)/d\cos\theta$	$0.0163(1 + 0.760\cos^2\theta)$
$d\sigma(e^+ + e^- \rightarrow \chi_{c2} + \delta_1)/d\cos\theta$	$0.0161(1 + 0.952\cos^2\theta)$
$d\sigma(e^+ + e^- \rightarrow \chi_{c2} + \delta_2)/d\cos\theta$	$0.00331(1 + 0.799\cos^2\theta)$
$d\sigma(e^+ + e^- \rightarrow \chi_{c2} + \delta_3)/d\cos\theta$	$0.00530(1 - 0.188\cos^2\theta)$

TABLE II: Differential cross sections–angular distribution functions for double charmonium production in  $e^+e^-$  annihilation at  $\sqrt{s} = 10.6$  GeV with both QCD and QED contributions (see text for the input parameters).

Differential cross section	Angular distribution function (fb)
$d\sigma(e^+ + e^- \rightarrow J/\psi + \eta_c(1S))/d\cos\theta$	$2.47(1 + \cos^2\theta)$
$d\sigma(e^+ + e^- \rightarrow J/\psi + \eta_c(2S))/d\cos\theta$	$1.62(1 + \cos^2\theta)$
$d\sigma(e^+ + e^- \rightarrow J/\psi + \eta_c(3S))/d\cos\theta$	$1.39(1 + \cos^2\theta)$
$d\sigma(e^+ + e^- \rightarrow J/\psi + \chi_{c0})/d\cos\theta$	$3.18(1 + 0.265\cos^2\theta)$
$d\sigma(e^+ + e^- \rightarrow J/\psi + \chi_{c1})/d\cos\theta$	$0.426(1 + 0.751\cos^2\theta)$
$d\sigma(e^+ + e^- \rightarrow J/\psi + \chi_{c2})/d\cos\theta$	$0.929(1 - 0.161\cos^2\theta)$
$d\sigma(e^+ + e^- \rightarrow J/\psi(1S) + {}^1D_2)/d\cos\theta$	$0.0770(1 + \cos^2\theta)$

TABLE III: Ratios of production cross sections of various double charmonia to that of  $J/\psi + \eta_c$  in  $e^+e^-$  annihilation at  $\sqrt{s} = 10.6$  GeV.

	$\eta_c(1S, 2S, 3S)$	$\chi_{c0}(1P, 2P)$	$\chi_{c1}(1P, 2P)$	$\chi_{c2}(1P, 2P)$	$h_c(1P, 2P)$	${}^3D_1$	${}^3D_2$	${}^3D_3$	${}^1D_2$
$\psi(1S)$	1.0,0.65,0.56	1.05,1.4	0.15,0.21	0.27,0.36					0.03
$\psi(2S)$	0.65,0.42,0.36	0.68,0.94	0.11,0.14	0.17,0.24					0.02
$\eta_c(1S)$					0.11,0.15	0.025			
$\eta_c(2S)$					0.07,0.10	0.016			
$\eta_c(3S)$					0.06,0.08				
$\chi_0(1P)$					0.03,0.05				
$\chi_1(1P)$					0.15,0.21	0.012	0.015	0.006	
$\psi_2(1P)$					0.010,0.013	0.006	0.001	0.0015	

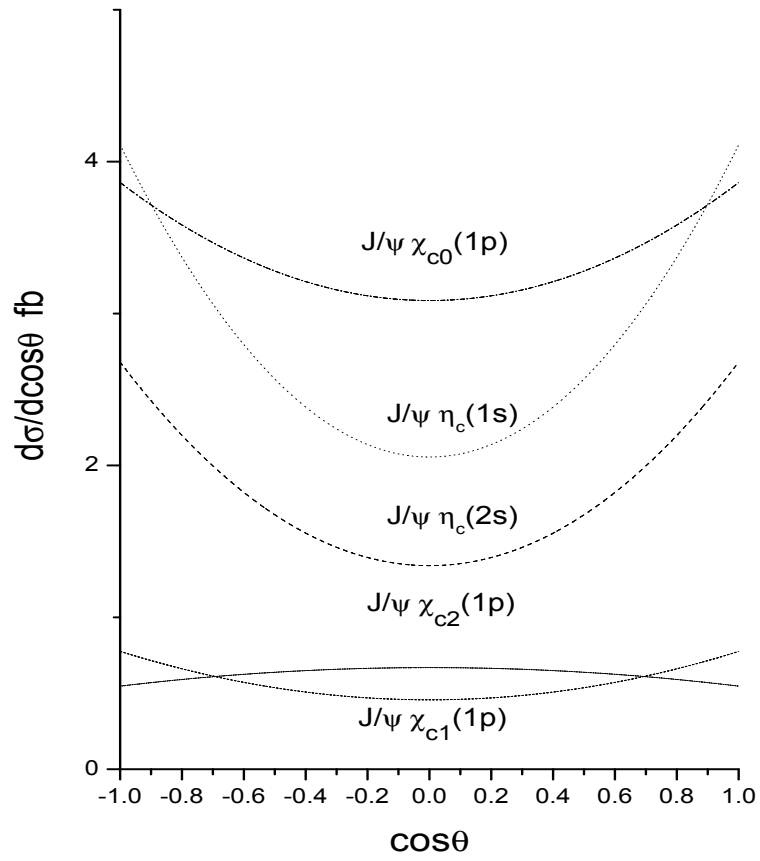


FIG. 1: Differential cross sections for  $e^+e^- \rightarrow J/\psi + \chi_{cJ}(\eta_c)$



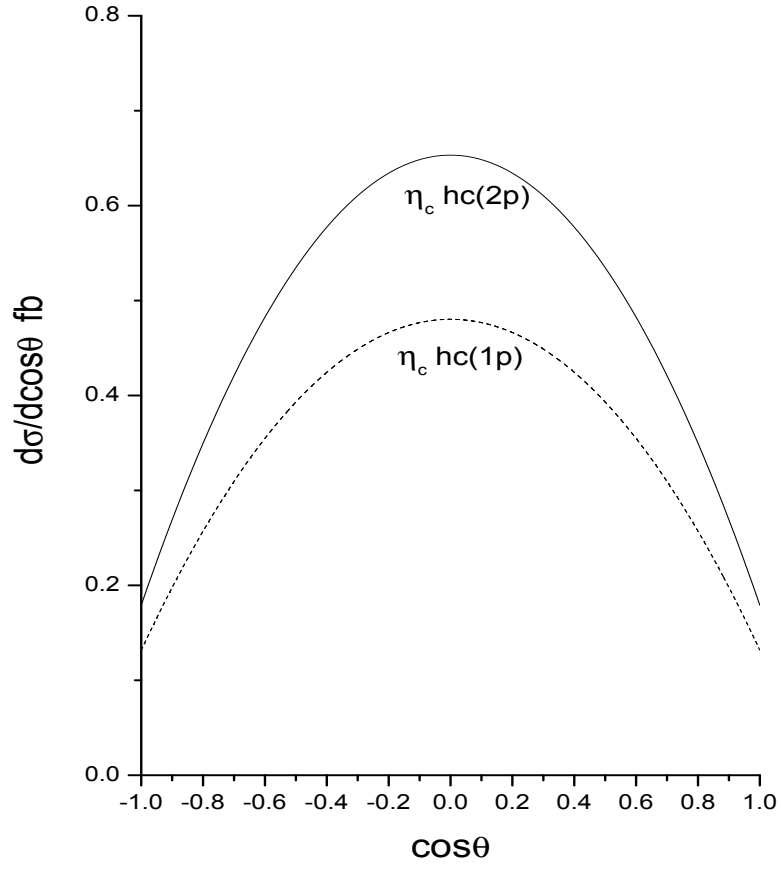


FIG. 2: Differential cross sections for  $e^+e^- \rightarrow \eta_c + h_c$

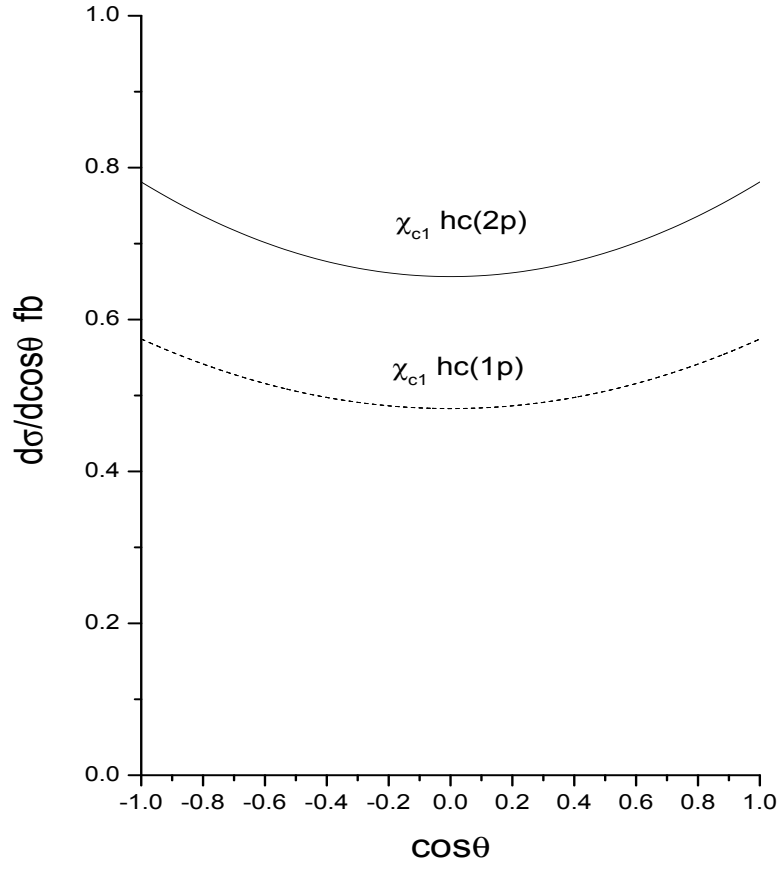


FIG. 3: Differential cross sections for  $e^+e^- \rightarrow \chi_{c1} + h_c$

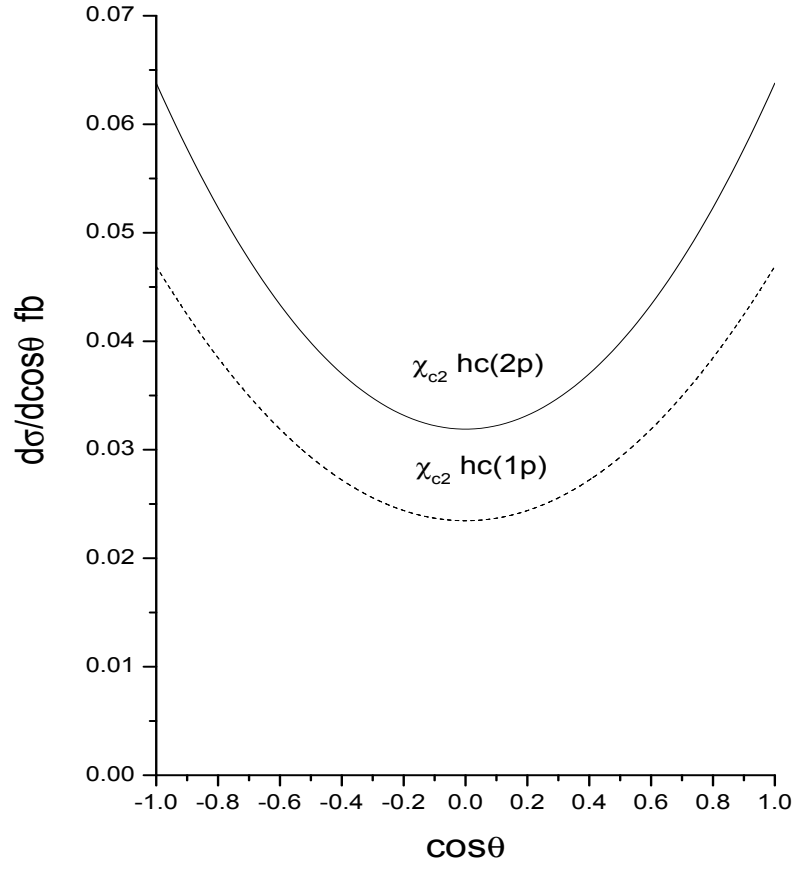


FIG. 4: Differential cross sections for  $e^+e^- \rightarrow \chi_{c2} + h_c$

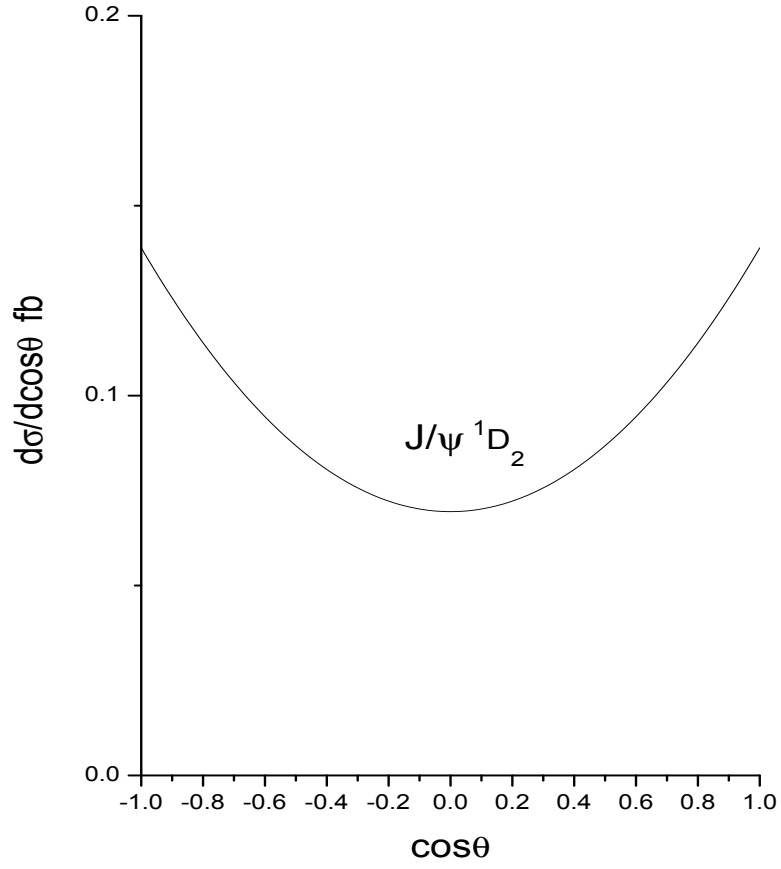


FIG. 5: Differential cross sections for  $e^+e^- \rightarrow J/\psi + {}^1D_2$

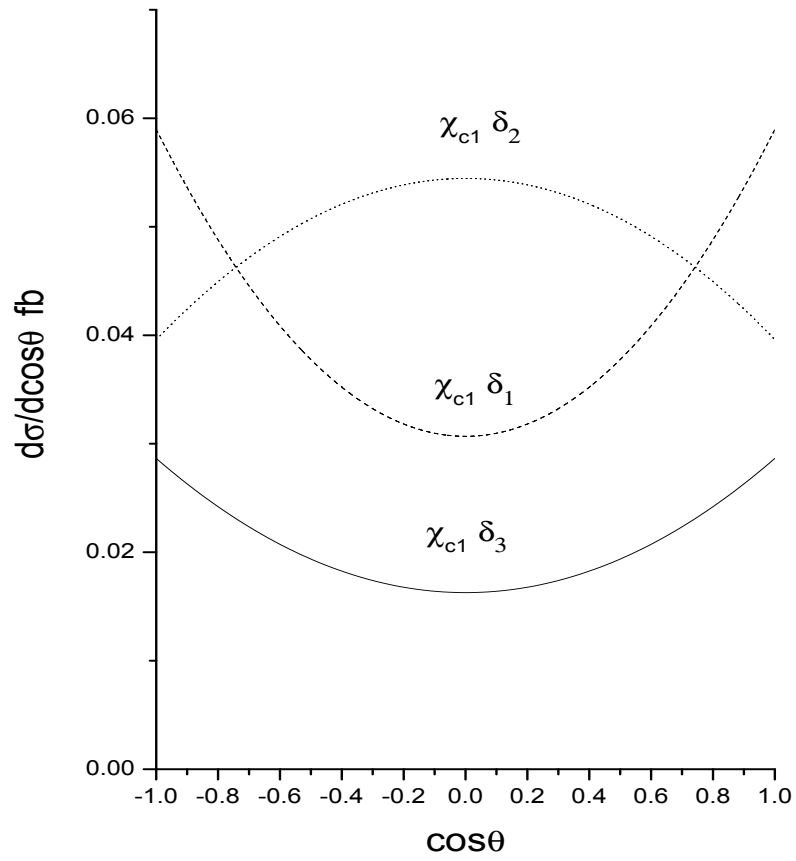


FIG. 6: Differential cross sections for  $e^+e^- \rightarrow \chi_{c1} + \delta_J$

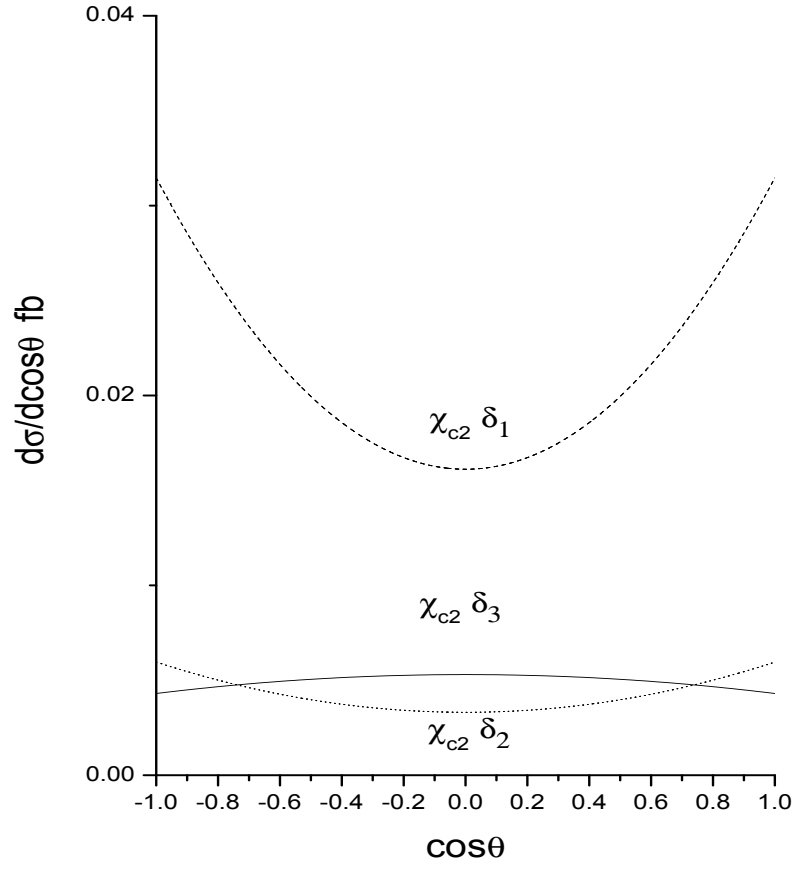


FIG. 7: Differential cross sections for  $e^+e^- \rightarrow \chi_{c2} + \delta_J$

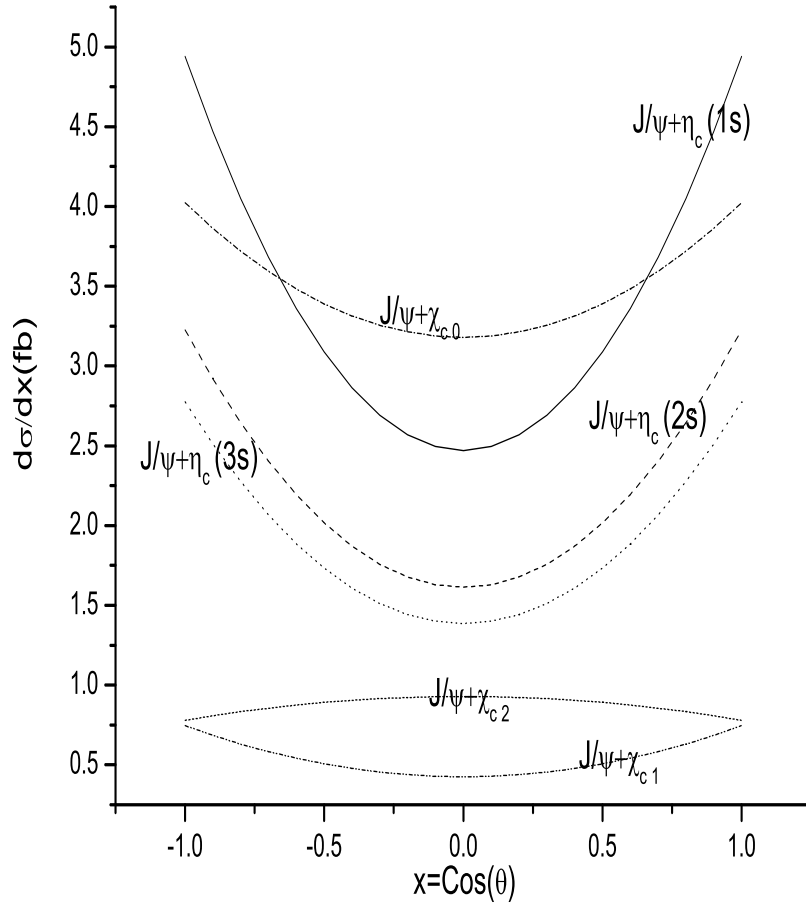


FIG. 8: Differential cross sections with both QCD and QED contributions for  $e^+e^- \rightarrow J/\psi\eta_c(1S, 2S, 3S)$  and  $e^+e^- \rightarrow J/\psi + \chi_{cJ}(J = 0, 1, 2)$